J. Fluid Mech. (1974), *vol.* 62, *part* 3, *pp.* 579–592
Printed in Great Britain

Convection induced by centrifugal buoyancy

By F. H. BUSSE AND C. R. CARRIGAN
Department of Planetary and Space Science, University of California, Los Angeles

(Received 22 June 1973)

The onset of convection is observed in a cylindrical annulus which is heated from the outside, cooled from the inside and rotating about its vertical axis of symmetry. The dynamical constraint exerted by the dominating Coriolis force inhibits the instability when the top and bottom boundaries of the annulus are conical so as to make the vertical height vary with distance from the axis. The experimental observations are in good agreement with the theoretical predictions by Busse (1970*a*). This confirmation indicates the absence of subcritical finite amplitude instabilities and suggests that the annulus experiment provides a close dynamical model for convection in the liquid core of the earth.

1. Introduction

Convection processes in stars and in the earth's core are governed by the fact that the direction of the buoyancy force does not, in general, coincide with the axis of rotation. While the case of coincidence can easily be realized in laboratory convection experiments, the presence of the earth's gravity seems to prevent the simulation of planetary and stellar convection processes under laboratory conditions. Inclining the rotation axis with respect to the vertical is not useful, since in this case gravity generates an oscillatory force in the rotating system. The centrifugal force appears to be the most easily realizable alternative source of buoyancy. Indeed, it is found to be ideally suited to simulate cases of geo- and astrophysical interest at high Taylor numbers, since in this case only the component of buoyancy perpendicular to the axis of rotation is of importance in a first approximation (Busse 1970*a*). Since the centrifugal force points away from the axis of rotation rather than towards it as gravity does in celestial bodies, the temperature gradient must also be outward. Hence, in order to induce convective instability in a fluid annulus rotating about its vertical axis, the outer boundary must be kept at a higher temperature than the inner boundary. Instability occurs when the fluid density difference between the boundaries is large enough for the centrifugal potential energy gained by exchanging fluid elements to overcome the effects of thermal and viscous dissipation and the possibly stabilizing influence of the Coriolis force.

It is the variety of effects by which the Coriolis force influences the dynamics of the convective flow which makes the experiment of convection in a cylindrical rotating annulus interesting even without geo- or astrophysical motivations. At high rotation rates the experiment strikingly exhibits the consequences of the Taylor–Proudman theorem. This theorem requires that nearly stationary motions

in a rapidly rotating fluid system be approximately independent of the co-ordinate z in the direction of the axis of rotation. Accordingly, the onset of convection occurs in the form of circulating rolls aligned parallel to the axis of rotation. In fact, in an infinitely long annulus this form of convection can be strictly independent of the z co-ordinate and the Taylor–Proudman theorem can be satisfied perfectly. The Coriolis force is balanced by the pressure gradient in this case and its inhibiting influence vanishes, with the result that the convection has the same properties as convection in a layer heated from below, except for the influence of the cylindrical geometry, which is minimized when the small-gap limit is considered.

The novel features of the annulus convection problem stem from the fact that the finite length of the annulus always requires the motion to be z dependent. Two effects are of importance. As long as the end surfaces are parallel to each other only the no-slip boundary condition for the tangential component of the velocity field enforces z dependence of the motion. This z dependence has the form of an Ekman boundary layer and is the dominant cause of viscous dissipation unless the ratio of length to gap width of the annulus becomes large. More important in the limit of high rotation rates is the case when the two end surfaces are not parallel. In this case the boundary condition for the normal component of the velocity enforces a z dependence. In contrast to the no-slip boundary condition this boundary condition holds even for an inviscid fluid and introduces a non-dissipative constraint. Since this constraint produces the most dramatic increase in the temperature difference necessary for the onset of convection we shall focus our attention on it in the experimental investigation.

The mathematical analysis of the various aspects of the convective instability in a rotating annulus has been presented in an earlier paper (Busse 1970*a*) hereafter referred to as I. This paper was restricted to a linear stability analysis which neglects effects caused by the finite amplitude of convection. An important question is whether nonlinear effects can overcome the constraints of rotation, and whether instability in the form of finite amplitude disturbances can occur at subcritical temperature gradients. The experimental observations indicate a negative answer to this question. They also show that the other assumptions made by the theory can be realized under laboratory conditions. In particular, the action of gravity, although comparable with the centrifugal force, has a negligible influence because of the horizontal character of the motions enforced by the Taylor–Proudman theorem.

Before describing the experiment we give a simplified theoretical analysis of the convective instability in § 2. For a more detailed discussion based on a different mathematical method we refer readers to I. The experimental apparatus and observational techniques are described in § 3. In § 4 the observations of the onset of convection are presented. Within the experimentally accessible range of parameters those cases are emphasized for which the various effects of rotation become most clearly distinguishable. The paper closes with remarks on the relevance of the experiment to the problem of convection in the earth's core and on aspects of the problem which should be the subject of future experiments.

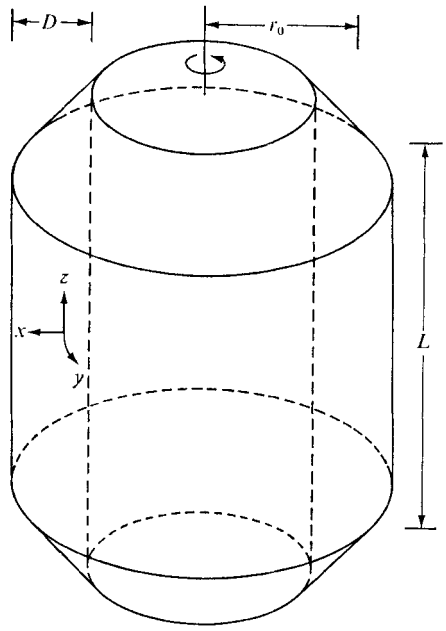

FIGURE 1. Geometrical configuration of the rotating annulus.

2. Convective instability induced by centrifugal buoyancy

We consider a cylindrical annulus filled with a homogeneous incompressible fluid and rotating with angular velocity Ω about its vertical axis of symmetry. The annular region is bounded by cylindrical surfaces with radii $r_0 \pm \frac{1}{2}D$ and by conical surfaces at both ends as shown in figure 1. Constant temperatures T_1 and T_2 with $T_2 > T_1$ are prescribed on the inner and outer cylinders, respectively, while the end surfaces are assumed to be insulators. Making the small-gap approximation $D \ll r_0$, we introduce a Cartesian system of co-ordinates with the origin at the centre of the annular channel and the x, y and z co-ordinates in the radial, azimuthal and vertical directions, respectively. In order to obtain a non-dimensional description of the problem we use L, Ω^{-1} and $(T_2 - T_1)\,L/D$ as scales for length, time and temperature, where L denotes the mean height of the annulus.

The non-dimensional Boussinesq equations of motion for the velocity vector $\hat{\mathbf{v}}$ and the heat equation for the temperature $\hat{\theta}$ are

$$E\nabla^2\hat{\mathbf{v}} - \nabla\hat{p} - B\left(\mathbf{i} - \mathbf{k}\frac{g}{\Omega^2 r_0}\right)\hat{\theta} = 2\mathbf{k}\times\hat{\mathbf{v}} + \hat{\mathbf{v}}.\nabla\hat{\mathbf{v}} + \frac{\partial\hat{\mathbf{v}}}{\partial t}, \tag{2.1a}$$

$$\nabla.\hat{\mathbf{v}} = 0, \tag{2.1b}$$

$$P^{-1}E\nabla^2\hat{\theta} = \hat{\mathbf{v}}.\nabla\hat{\theta} + \partial\hat{\theta}/\partial t, \tag{2.1c}$$

where

$$E \equiv \nu/\Omega L^2$$

is the Ekman number, $P \equiv \nu/\kappa$ is the Prandtl number and

$$B = \gamma(T_2 - T_1)\,r_0/D \tag{2.2}$$

is the buoyancy parameter. ν, κ and γ are kinematic viscosity, thermometric conductivity and expansion coefficient, respectively. $\mathbf{i}$, $\mathbf{j}$ and $\mathbf{k}$ are unit vectors in the x, y and z directions, and g is the acceleration due to gravity in the direction opposite to $\mathbf{k}$.

In the case when gravity is negligible compared with the centrifugal force equations (2.1) have the solution

$$\hat{\mathbf{v}} = 0, \tag{2.3a}$$

$$\hat{\theta} = (T_2+T_1)\,D/2(T_2-T_1)\,L+x. \tag{2.3b}$$

More realistic in the laboratory experiment is the case when the two body forces are of the same order of magnitude. The temperature distribution (2.3*b*) does not change in this case, however, provided that E is sufficiently small, because an azimuthal velocity field in the form of a thermal wind is realized in the interior of the annulus. We shall disregard this velocity field in the following, since it has been shown in I that it has a negligible influence on the convective instability.

In order to investigate the stability of the basic solution (2.3), we superimpose infinitesimal disturbances $\mathbf{v}$ and θ with exponential y and t dependences:

$$\mathbf{v}, \theta \propto \exp\{i\alpha y + i\omega t\}.$$

Of interest is the case of marginal stability characterized by the vanishing of the imaginary part of ω. The stability depends strongly on the boundary conditions at the conical boundaries, given by

$$z = \tfrac{1}{2}-\eta_T x, \quad z = -\tfrac{1}{2}+\eta_B x. \tag{2.4}$$

We shall assume η_T, $\eta_B \ll 1$, corresponding to a slight inclination of the boundaries. The condition that the tangential component of the velocity field vanishes at the boundaries (2.4) leads to the formation of Ekman layers which do not need to be considered explicitly if the condition for the normal component of the velocity field is modified by an influx of order $E^{\frac{1}{2}}$ (Greenspan 1968, p. 92):

$$\mathbf{v}.\mathbf{k} = \left\{ \begin{array}{lll} -\eta_T \mathbf{v}.\mathbf{i} - \tfrac{1}{2}E^{\frac{1}{2}}\mathbf{k}.\nabla\times\mathbf{v} & \text{at} & z = \tfrac{1}{2}, \\ \eta_B \mathbf{v}.\mathbf{i} + \tfrac{1}{2}E^{\frac{1}{2}}\mathbf{k}.\nabla\times\mathbf{v} & \text{at} & z = -\tfrac{1}{2}. \end{array} \right\} \tag{2.5}$$

The boundary conditions at the side walls are of lesser importance and will be discussed later.

The solution of the equations of motion for $\mathbf{v}$ is based on the presumption that in the first approximation the flow is governed by the geostropic balance

$$2\mathbf{k}\times\mathbf{v} \approx -\nabla p, \tag{2.6}$$

which requires that E as well as B and ω be small numbers. Oscillations with ω of the order unity are possible but not relevant to the stability problem, as has been shown in I. The balance (2.6), together with the condition $\nabla.\mathbf{v} = 0$, is satisfied by

$$\mathbf{v} \approx -\tfrac{1}{2}\nabla\times\mathbf{k}p(x)\,e^{i\alpha y+i\omega t}, \tag{2.7}$$

where the radial dependence of the pressure remains undetermined. Since we have chosen the flow to be normal to $\mathbf{k}$ the boundary condition (2.5) is also

approximately satisfied. By taking the curl the geostropic balance can be eliminated from the equation of motion:

$$E\nabla^2\nabla\times\mathbf{v}-B\nabla\theta\times(\mathbf{i}-\mathbf{k}g/\Omega^2r_0)=-2\mathbf{k}.\nabla\mathbf{v}+i\omega\nabla\times\mathbf{v}. \tag{2.8}$$

We multiply this equation, which contains only terms of small order, by $\mathbf{k}$ and take the average over the z co-ordinate, which will be indicated by a bar. Using (2.5) we obtain

$$\mathbf{k}.\nabla\times\{E\overline{\nabla^2\mathbf{v}}-i\omega\bar{\mathbf{v}}\}+\mathbf{j}.\nabla\bar{\theta}=[2\eta_T\mathbf{v}.\mathbf{i}+E^{\frac{1}{2}}\mathbf{k}.\nabla\times\mathbf{v}]_{z=\frac{1}{2}}+[2\eta_B\mathbf{v}.\mathbf{i}+E^{\frac{1}{2}}\mathbf{k}.\nabla\times\mathbf{v}]_{z=-\frac{1}{2}}. \tag{2.9}$$

We shall replace the average $\bar{\mathbf{v}}$ as well as the horizontal component of $\mathbf{v}$ at the boundary by the approximate solution (2.7). Further, we eliminate $\bar{\theta}$ by using the heat equation

$$P^{-1}E\nabla^2\theta=\mathbf{i}.\mathbf{v}+i\omega\theta, \tag{2.10}$$

and obtain for the as yet undetermined function $p(x)$

$$\left[EP^{-1}\left(\frac{d^2}{dx^2}-\alpha^2\right)-i\omega\right]\left\{\left[E\left(\frac{d^2}{dx^2}-\alpha^2\right)-2E^{\frac{1}{2}}-i\omega\right]\times\left(\frac{d^2}{dx^2}-\alpha^2\right)+2i\alpha(\eta_T+\eta_B)\right\}p=-\alpha^2Bp. \tag{2.11}$$

Equation (2.11) allows us to discuss the two different ways in which the Coriolis force influences the onset of convection: the Ekman boundary-layer dissipation and the change in height owing to a non-vanishing value of $\eta_T+\eta_B$. We shall also include the case where viscous dissipation in the interior exceeds the other terms; i.e. $(L/D)^4E\gg1$. In this latter case, (2.11) reduces to the equation for convection in a layer heated from below without rotation. Using rigid boundaries at $x=\pm D/2L$ we find as the critical value of B for the onset of convection (see, for example, Chandrasekhar 1961, chap. 2)

$$B_c=1708E^2P^{-1}(L/D)^4 \quad \text{for} \quad E^{-\frac{1}{2}}\ll L/D. \tag{2.12}$$

$BE^{-2}P(D/L)^4$ is the Rayleigh number used in ordinary convection. When E becomes small compared with $(D/L)^4$ and the change in height can be neglected, the friction in the Ekman boundary layer becomes the dominant stabilizing force, yielding the critical value

$$B_c=8(\pi L/D)^2E^{\frac{3}{2}}P^{-1} \quad \text{for} \quad E^{-\frac{1}{4}}\gg L/D, \tag{2.13}$$

as has been shown in I. If a small but finite value of $\eta_T+\eta_B$ exists the variation of height becomes the main constraint in the limit of large rotation rates. Viscous dissipation is required to balance this constraint, which would lead to convection with infinitely small wavelengths in an inviscid fluid. When $(\eta_T+\eta_B)P$ is much larger than $E^{\frac{1}{4}}$ viscous dissipation in the interior is much more effective in providing the balance than is Ekman-layer dissipation. Neglecting the latter, we obtain from (2.11) as the critical value for B

$$B_c=3\left\{4PE^2\left(\frac{\eta_T+\eta_B}{1+P}\right)^4\right\}^{\frac{1}{3}} \quad \text{for} \quad (\eta_T+\eta_B)P\gg E^{\frac{1}{4}}. \tag{2.14}$$

In contrast to the cases discussed above, ω does not vanish in the present case:

$$\omega = -2(\eta_B+\eta_T)/\alpha_c(1+P). \tag{2.15}$$

In deriving (2.14) and (2.15) it has been assumed that

$$L\pi/D \ll \{(\eta_B+\eta_T)\,P/E(1+P)\}^{\frac{1}{3}}, \tag{2.16}$$

in which case the azimuthal dependence of convection dominates the radial dependence. The critical wavenumber α_c is given by

$$\alpha_c = \{2^{\frac{1}{2}}(\eta_B+\eta_T)\,P/E(1+P)\}^{\frac{1}{3}}. \tag{2.17}$$

Because of the low power of E in (2.14) the effect of height variation can most easily be isolated experimentally from the other effects. It is also the most interesting of the three mechanisms since it is associated with a time dependence and a differential rotation, although the latter phenomenon has not yet been investigated theoretically or experimentally. Of particular interest is the fact that the onset of convection does not depend on the thickness D of the annulus if the temperature gradient is kept constant. This is a remarkable feature if it is remembered that convection in a layer heated from below depends on the fourth power of the layer thickness. In the latter case the release of potential energy associated with the vertical velocity component is opposed by viscous and thermal dissipation, which inhibits motions with high wavenumbers. In the present case the release of potential energy is primarily opposed by the variation of height, which does not depend on the wavenumber. Hence the maximization of the buoyancy force leads to the high azimuthal wavenumber (2.17) and the negligible role of the radial scale D.

3. Experimental apparatus and observational method

The experimental apparatus which was constructed to observe convection in a rotating annulus closely reproduces the configuration considered in the previous section. A vertical cross-section of the apparatus is shown in figure 2. The coaxial cylinders are rigidly mounted on two circular end plates. A temperature gradient across the annular gap is established by circulating cool water on the inside of the inner cylinder and surrounding the outer cylinder by warm water. In order to avoid optical distortions this latter step is accomplished by enclosing the annulus in a watertight rectangular box made of acrylic plastic. Warm water from a thermostatically controlled reservoir is circulated through an inlet and an outlet at opposite corners of the box. It is more difficult to provide water of constant temperature inside the rotating annulus. For this purpose two centred hollow shafts mounted on the circular end plates serve as inlet and outlet for the circulating coolant and, at the same time, as the rotation axis. Attached to the inside of the end plates are baffles to ensure an efficient distribution of the coolant at the wall of the inner cylinder. Ball-and-socket couplings are used on both ends to connect the shafts to the tubes coming from and returning to the thermostatically controlled coolant reservoir. Finally, figure 2 shows the copper–constantan thermocouple used to measure the temperature difference between the inner and outer baths.

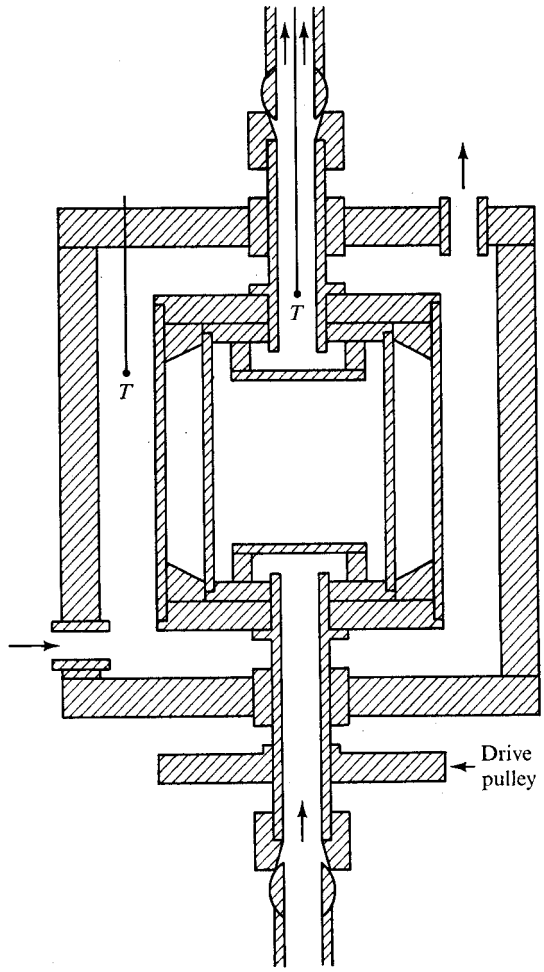

FIGURE 2. Schematic diagram of the experimental apparatus. T, thermocouple.

For the purpose of visual observation the outer cylinder was made of acrylic plastic, while aluminium tubing was used for inner cylinders of two different sizes. In order to emphasize the role of the Coriolis force and to avoid too small temperature differences at the onset of convection the inner diameter of the annulus was kept at the rather small value of about 9 cm. Rotation rates up to 400 r.p.m. were achieved with a variable-speed motor, resulting in centrifugal forces up to $7g$. In most cases the fluid in the annular region was water. For the purpose of visualization a small amount of a solution with suspended nearly neutrally buoyant particles (AQ 1000, Kalliroscope Corp.) was added to the fluid. As soon as shearing motions occur in the fluid the flaky particles become aligned with the shear. Because of non-homogeneous reflexion the pattern of the shear becomes visible when a stroboscopic light source (Strobotac^{R}, General Radio Co.) is used. The onset of convection was determined by observing the annulus at a given temperature difference for discrete values of the rotation rate. Since

spurious patterns are sometimes generated by the spin-up process and since the growth rate of the convective instability is small in the neighbourhood of the critical value, the experimental conditions were kept constant for at least 10 min before it was decided whether or not columns indicating convection rolls were present. A much longer waiting period of the order of 40 min was used when the temperature difference was changed to a new value. The critical point was approached in general both from above and below. No noticeable difference was found within the accuracy of observations. The very fact that columns become visible only at finite amplitudes of motion causes an overestimate of the critical value B_c of the buoyancy parameter. In most cases, however, this error did not seem to exceed the magnitude of the other systematic errors.

Typical sources of experimental errors are the measurement of the temperature and the determination of the rotation rate. Since the difference $T_2 - T_1$ for the onset of convection amounts to only a fraction of a °K, large thermostatically controlled reservoirs (0·07 m^3 and 0·2 m^3) and a high circulation rate (0·015 m^3/min) were used to ensure that the temperature difference varied by less than 0·03 °K. On a time scale of a few minutes, however, the variation was considerably less and by carefully monitoring the temperature difference the estimated error in its determination was kept below 0·01 °K.

The rotation rates were measured with the stroboscope, which indicated slow drifts of 2–3 % on the time scale of a single experiment. Other uncertainties were introduced by inaccuracies and changes in the material properties. In particular, the outer cast acrylic cylinder seemed to change heat conductivity after long periods of submersion in water. In order to investigate this effect, the acrylic cylinder was replaced by a glass cylinder in some of the experiments. The measurements of the onset of convection did not show any noticeable difference, however. This fact seems to indicate that the critical value of the buoyancy parameter does not depend strongly on the temperature condition at the boundary, which is reassuring, since the theoretical boundary condition of a prescribed temperature is not well approximated in the experiment because of the finite thickness ($\sim$ 0·3 cm) of the outer wall. The drop in the imposed temperature difference across the wall has always been taken into account in the calculation of B. The tolerance of about 0·03 cm in the gap width of the annulus introduces an additional source of error. We have represented the data without error bars since the apparent scatter of the data gives a reasonable indication of the uncertainties.

4. Experimental results

In view of the large number of parameters in the general case, the experimental investigations have emphasized those cases in which the onset of convection is predicted approximately by one of the three simple relations for the critical value B_c given in § 2. Because of experimental limitations it has not always been possible to separate the three different stabilizing mechanisms sufficiently well. This is true particularly in the case of the Ekman-layer dissipation, when the theoretical curve should be regarded as a guideline rather than an actual prediction.

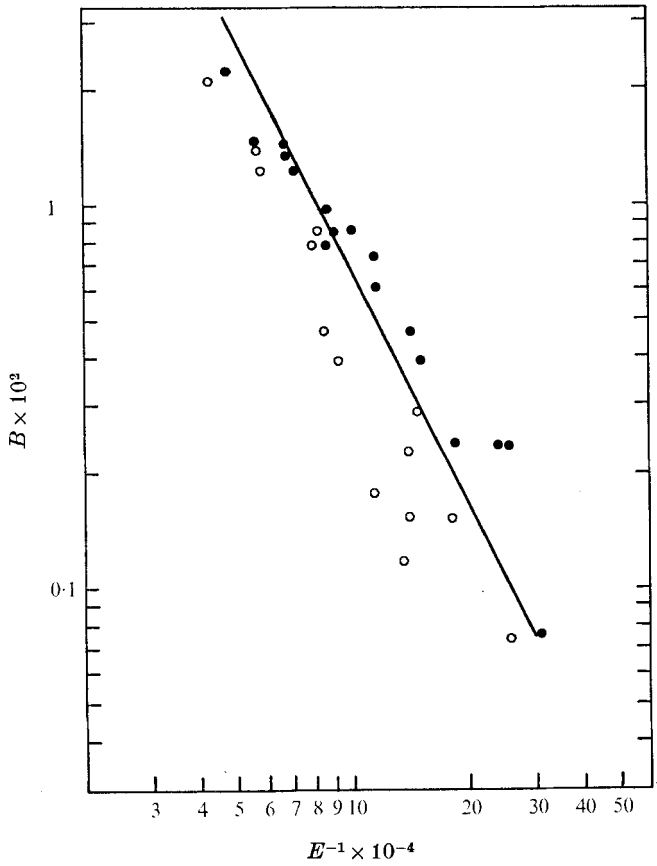

FIGURE 3. Onset of convection in the case when interior dissipation dominates. The theoretical line represents relation (2.12). The dimensions of the annular region are $L = 28{\cdot}6$ cm, $D = 0{\cdot}6$ cm, $r_0 = 13{\cdot}64$ cm. The fluid is 10 c St silicon-oil (Dow Corning 200 Fluid). In this and the following figures filled circles indicate observation of convection columns; open circles indicate that no convection was observed.

We start with the simple case of dominating interior dissipation. It can be easily realized experimentally by choosing a high enough aspect ratio L/D. Actually, a larger cylinder than that described in § 3 was used for the measurements shown in figure 3. The fact that the onset of convection occurs for low rotation rates at smaller values of B than those predicted by (2.12) is probably caused by baroclinic effects and the fact that the shear of the cubic profile of the basic axisymmetric flow contributes to instability. The latter influence is indicated by the observation that the convection columns show a slight ($\approx 10°$) deviation from the vertical in the sense of a helix spiralling upward in the direction opposite to that of the rotation. This property is in accordance with the well-known fact (Busse 1970c; Joseph & Munson 1970) that the onset of shear-flow instabilities in a rotating system occurs in such a way that the components of the curl of the shear and of the rotation vector perpendicular to the axis of the convection roll have opposite signs.

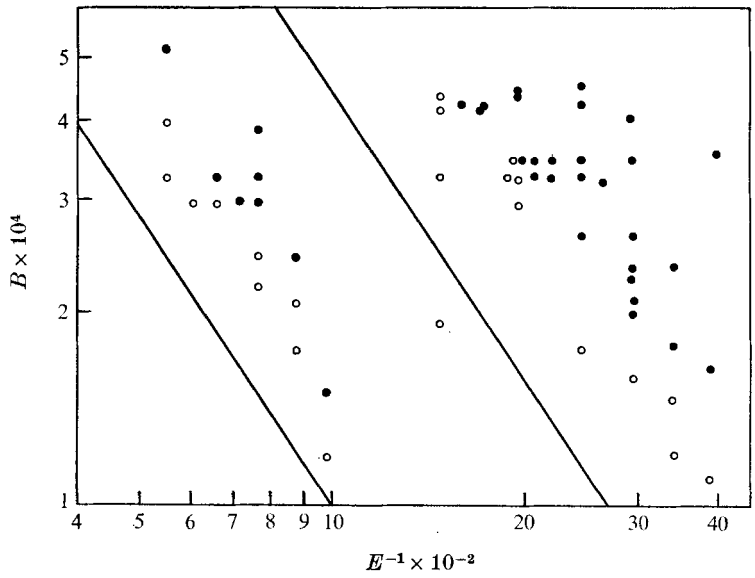

FIGURE 4. Onset of convection for $D = 0{\cdot}97$ cm, $r_0 = 4{\cdot}29$ cm, with horizontal top and bottom plates. $L = 0{\cdot}95$ cm in the case of the data on the right and $L = 0{\cdot}45$ cm for data on the left side. The theoretical lines represent expression (2.13). Water at a mean temperature of 30 °C was used in this and the following experiments.

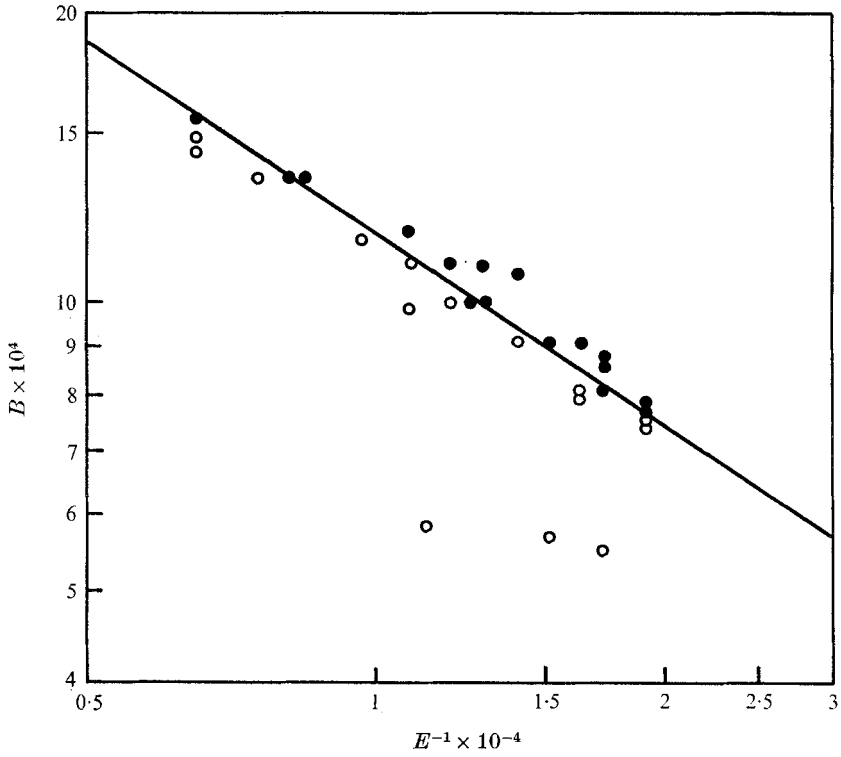

FIGURE 6. Onset of convection in the case of varying height with $\eta_T = \eta_B = \tan 22{\cdot}5°$, $L = 1{\cdot}96$ cm, $D = 0{\cdot}97$ cm, $r_0 = 4{\cdot}29$ cm. The theoretical line represents expression (2.14).

In order to observe the onset of convection in the case when the Ekman-layer dissipation is the dominant feature, it became necessary to use rather small values of L down to a value of less than 0·5 cm. In this case, the method of observation of the columns is rather cumbersome, and it may be that the critical value B_c is overestimated by the observations more than in the other cases. However, the data presented in figure 4 clearly show the approach to the theoretical line as L/D decreases.

Particular attention has been devoted to the case of changing height. The stabilizing influence of this case can be strikingly demonstrated by combining the changing-height case and the constant-height case into one annulus, as shown in figure 5 (plate 1). While strong convection columns are visible in the latter case the axisymmetric state is still stable in the first case.

Figure 6 shows the observations of instability when the top and bottom surfaces are inclined at 22·5° to the horizontal. The experimental data agree well with the theoretical expression (2.14) for $\eta_T = \eta_B = \tan 22{\cdot}5° = 0{\cdot}4142$. Even for larger inclinations the theoretical formula predicts the onset of instability quite well, as shown in figure 7 (*a*), which shows the result for 45° cones. This is a surprising result in view of the fact that the theoretical expression was derived under the assumption of small inclinations. The experiment suggests that the horizontal component of the velocity field at the boundary is well represented by (2.7) for η of order unity. That the perturbation result may still be applicable in this case is also suggested by the fact that the buoyancy, viscous force and time dependence still give terms in the equation of motion (2.1*a*) small in comparison with the Coriolis force.

It has been emphasized earlier that a striking feature of expression (2.14) is the property that for a given temperature gradient the onset of convection is independent of the width of the annulus. This prediction has been tested by repeating the experiment with 45° cones for a gap width increased by 60%. For high rotation rates the onset of convection as shown in figure 7 (*b*) is indeed undistinguishable from that for the small gap width within experimental accuracy, while at low rotation rates the expected destabilizing effect of the increased width becomes noticeable.

A number of additional experiments have been performed which are not presented here since they correspond to cases in which the general equation of the theory does not reduce to the simple asymptotic expressions (2.12), (2.13) and (2.14). Since these expressions govern the important effects it is of lesser interest to relate experiment and theory in more general cases. In a number of representative cases the experiment was also performed with a reversed temperature gradient in order to establish the convective origin of the instability in contrast to the baroclinic instability, which does not depend on the centrifugal force. Within the range of parameters used for the experiments described above, no instability was found, in agreement with the theoretical expectation expressed in I.

Qualitative observations of the wavelength and phase velocity have been made in the case of changing height. The decrease of the wavelength with increasing rotation rate was clearly noticeable and the phase velocity was estimated from

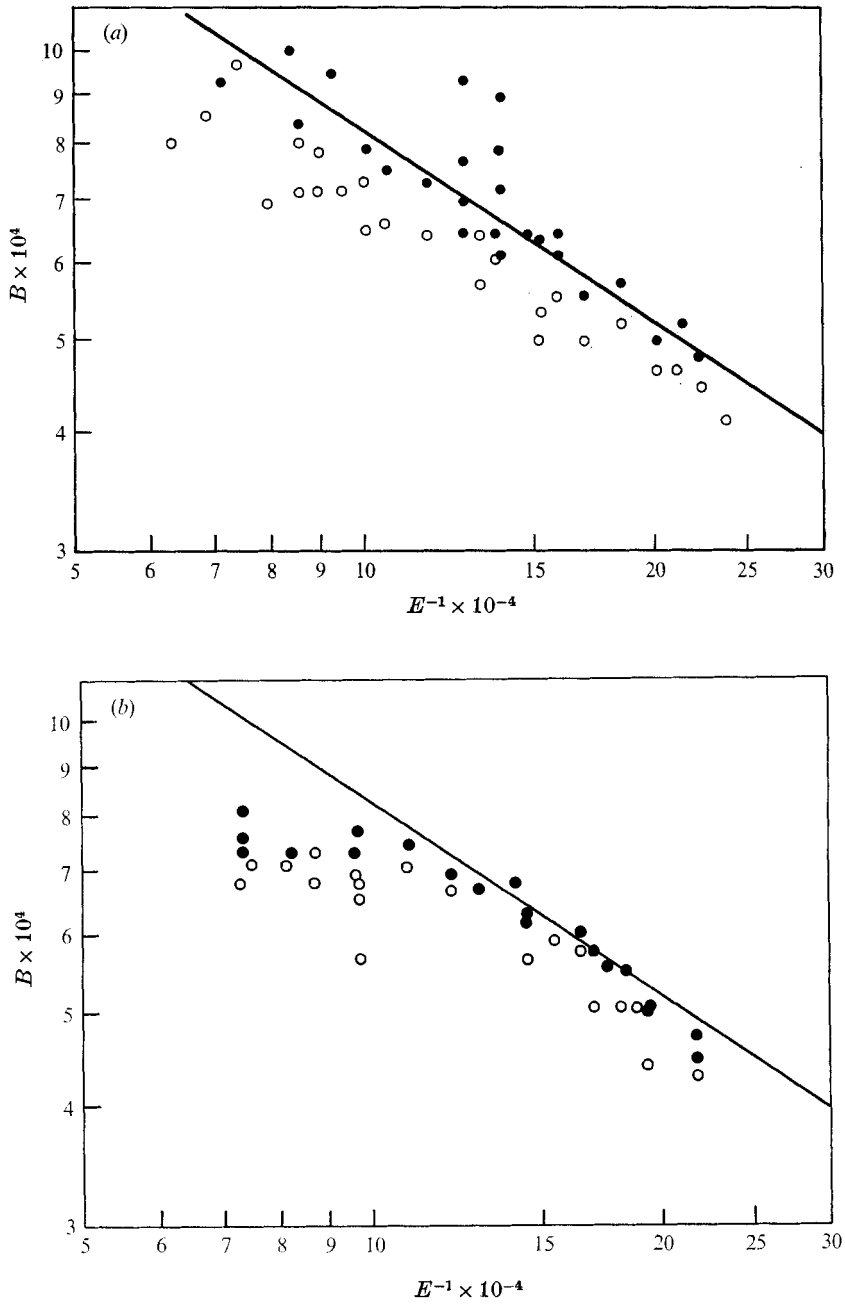

FIGURE 7. Onset of convection for $\eta_T = \eta_B = \tan 45°$. The theoretical line represents expression (2.14). (*a*) $D = 0{\cdot}97$ cm, $r_0 = 4{\cdot}29$ cm, $L = 6{\cdot}98$ cm. (*b*) $D = 1{\cdot}56$ cm, $r_0 = 3{\cdot}96$ cm, $L = 6{\cdot}69$ cm.

the propagation rate of the visible columns. However, the convective instability typically did not occur in the form of a single individual wave, but rather in the form of a superposition of several waves. Accordingly, the columns showed beating phenomena and only crude results could be obtained by visual observations. Qualitatively the results agreed with expressions (2.15) and (2.17), although the observations tended to show smaller values for the frequency ω as well as for the wavenumber α. In future experiments, which will be directed towards nonlinear phenomena, we shall also attempt to employ measuring devices to determine quantitatively the amplitude of convection as the columns pass by a particular point of the wall.

5. Concluding remarks

The good agreement found between the observations and the theoretical predictions permits the conclusion that the centrifugally induced convective instability is adequately described by linear theory. In a sense it is surprising that no finite amplitude mechanism of instability appears to have been observed in the experiment. The nonlinear terms in the equation of motion allow subcritical onset of instability in many situations where a strong constraint inhibits the growth of infinitesimal disturbances. An example of this phenomena is the onset of subcritical finite amplitude convection in a layer heated from below and rotating about a vertical axis (Veronis 1968).

The validity of the linear stability theory in the laboratory experiment encourages its application to the problem of convection in the earth's core. If thermal convection does indeed occur in the core, the critical condition for the onset of instability derived in I and corresponding essentially to expression (2.11) imposes strong constraints on the values of the physical parameters. The theory remains essentially applicable in the case of non-thermal convection caused by the sinking of solid particles (Busse 1972; Malkus 1973). In the case of convection in a layer heated from below, nonlinear aspects of convection such as convective heat transport have been successfully described by perturbation solutions based on the linear results. The experimental observations indicate that such an analysis is likely to succeed as well in describing the nonlinear properties of convection in an annulus. One of the particularly intriguing nonlinear features is the differential rotation generated by convection in the case of changing height. This phenomenon has been analysed by the perturbation method in the case of a slowly rotating spherical convection layer (Busse 1970*b*, 1973), and a similar analysis can be done without difficulty in the asymptotic case of high rotation rates considered in the present paper. Corresponding measurements of the differential rotation in a modified experiment are planned which will allow us to demonstrate this important geo- and astrophysical phenomenon in the laboratory.

The authors are indebted to the late Paul Cox for his skilful construction of the apparatus. The research was supported by the National Science Foundation under Grant GA-31247.

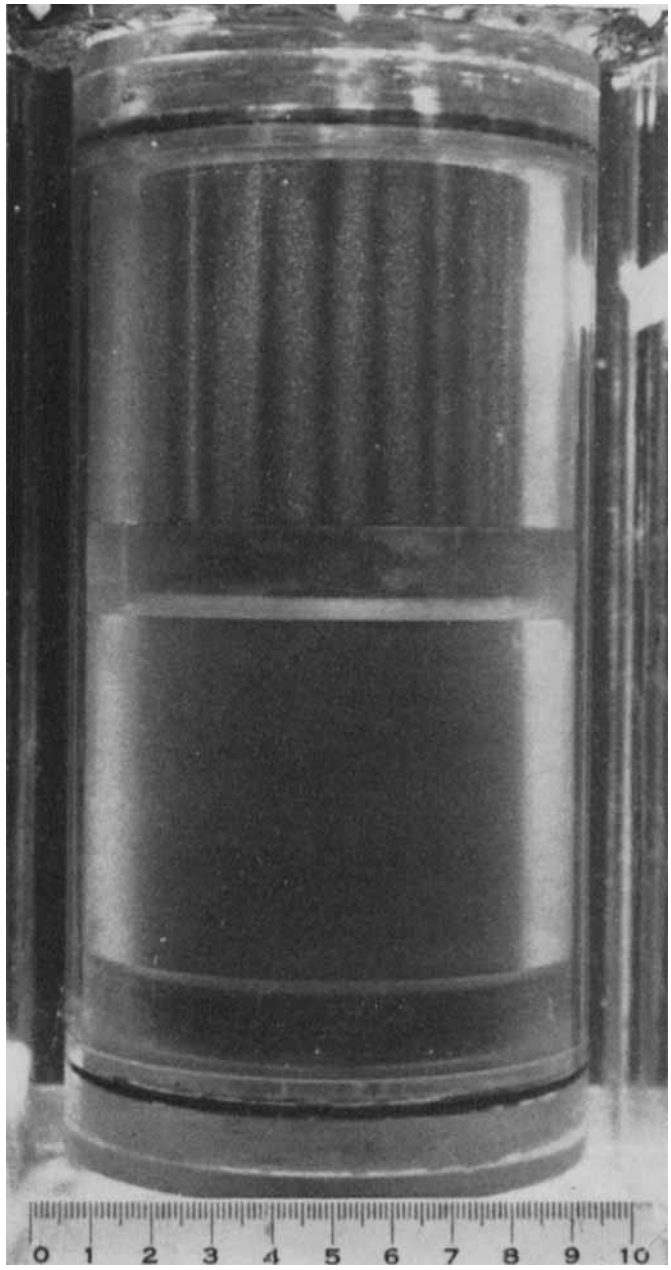

FIGURE 5. The experimental apparatus with an annulus of constant height in the upper part and an annulus with conical end surfaces in the lower part. The stabilizing effect of the variation in height is evident from the fact that strong convection columns are seen in the upper annulus while the lower annulus is stable. Scale in cm.

REFERENCES

BUSSE, F. H. 1970*a* *J. Fluid Mech.* **44**, 441.

BUSSE, F. H. 1970*b* *Astrophys. J.* **159**, 629.

BUSSE, F. H. 1970*c* *Z. angew. Math. Mech.* **50**, T173.

BUSSE, F. H. 1972 *J. Geophys. Res.* **77**, 1589.

BUSSE, F. H. 1973 *Astron. Astrophys.* **28**, 27.

CHANDRASEKHAR, S. 1961 *Hydrodynamic and Hydromagnetic Stability*. Oxford University Press.

GREENSPAN, H. P. 1968 *The Theory of Rotating Fluids*. Cambridge University Press.

JOSEPH, D. D. & MUNSON, B. R. 1970 *J. Fluid Mech.* **43**, 545.

MALKUS, W. V. R. 1973 *Geophys. Fluid Dyn.* **4**, 267.

VERONIS, G. 1968 *J. Fluid Mech.* **31**, 113.